Coastal Dynamics 2017
Paper No. 167

Beach evolution and recovery from a sequence of extreme storms

Olivier Burvingt[1], Gerd Masselink[1], Paul Russell[1] and Tim Scott[1]

Abstract

The impact of extreme storms on beaches typically causes rapid reductions in beach volume. There is considerable interest in how long recovery takes because, where recovery is slow, the coast will be less resilient to further storm impact. Many beaches along the southwest coast of England experienced large volumetric changes during the 2013/14 winter, considered as the most energetic wave conditions in the region since at least 1948. A 10-year beach volume time-series of 16 study sites corresponding to four different storm response types was analysed. It showed that the 2013/14 storms accounted for the largest volumetric changes for the last 10 years, and that many of the most affected beaches showed only partial recovery two years later. The weak recovery was mainly attributed to the relatively energetic winter wave conditions in 2015 and 2016. The comparison between the different beach volume time-series also highlighted the existence of beach behaviour that is relatively coherent at a multi-annual scale along the north coast of Cornwall.

Key words: multi-annual beach evolution, extreme storms, beach recovery, exposed beach, beach rotation, regional beach behaviour.

1. Introduction

Multi-annual and decadal time-series of shoreline or beach volume evolution are available around the world (Pye and Blott, 2008; Corbella et al., 2012; Barnard et al., 2015; Masselink et al., 2016; Scott et al., 2016; Splinter et al., 2016; Turner et al., 2016; Castelle et al., 2017; Phillips et al., 2017). In regions where wave climates are seasonally rhythmic, these time-series generally consist in alternating periods of erosion during winters and accretion during summers (Masselink et al., 2016; Scott et al., 2016; Splinter et al., 2016; Turner et al., 2016; Castelle et al., 2017). The episodic nature of extreme events has significant impacts on beach and shoreline long-term evolution (Pye and Blott, 2008; Masselink et al., 2015). The recovery processes following these extreme events have been widely studied, and recovery can take place within days (Birkemeier, 1979; Poate et al., 2015), months (Yu et al., 2013; Phillips et al., 2017), years (Choowong et al., 2009; Corbella et al., 2012; Suanez et al., 2012; Castelle et al., 2017) or even decades (Thom and Hall, 1991; Houser et al., 2015). The rapidity and the efficiency of these recovery processes are dependent on many factors, particularly general wave conditions and wave climate (Pye and Blott, 2008; Barnard et al., 2015; Masselink et al., 2016; Scott et al., 2016; Splinter et al., 2016), but also on the severity of the storm and the beach response mechanisms (Corbella et al., 2012; Scott et al., 2016), the antecedent beach state (Voudoskas et al., 2012), and morpho-dynamic relationships between the beach and the intertidal/subtidal bar (Houser et al., 2015; Brooks et al., 2017; Phillips et al., 2017) -and/or aerial dune systems (Suanez et al., 2012; Houser et al., 2015).

The southwest (SW) coast of England is generally subject to extra-tropical storms during winter periods (from November to March). During the 2013/14 winter, wave conditions were recognized as the most energetic since at least 1948 (Masselink et al., 2016), causing significant geomorphological change along the coastline (Masselink et al., 2015; Scott et al., 2016; Burvingt et al., 2016).

Analysis of a pre- and post-storm airborne LiDAR dataset over 157 highly diverse beaches in SW England classified four types of beach response to the 2013/14 extreme storms based on net volumetric change and alongshore morphological variability (Burvingt et al., submitted). The four storm response types each

[1]School of Biological and Marine Sciences, Plymouth University, UK. olivier.burvingt@plymouth.ac.uk

represented a distinctive morphological response, as follows: (1) fully exposed beaches that experienced large alongshore-uniform sediment losses; (2) semi-exposed beaches that experienced medium alongshore-uniform sediment losses; (3) sheltered short beaches that experienced limited alongshore variability in beach response, but limited net sediment change; and (4) sheltered long beaches that experienced considerable alongshore variability in beach response, but limited net sediment change. These four storm response types were used to select the 16 study sites presented in this paper.

Benefitting from the continuous collection of topographic data for the last 10 years, this study aims firstly to contextualize the extreme storms of the 2013/14 winter over the last decade and secondly to discuss the recovery processes following the extreme storm erosion. Wave conditions are then analysed to help interpret the regional variability among the 16 study sites that corresponded to the four different types of beach response to the 2013/14 extreme storms.

2. Study area and datasets

2.1. *Study area*

The SW coast of England has a wide variety of beach types, geological boundaries and hydrodynamic conditions (Scott et al., 2011), including long and wide sandy beaches, gravel barriers, small pocket beaches and beaches backed by extensive dunes systems or high rocky cliffs. For this study, 16 beaches are considered and are numbered sequentially in an anti-clockwise direction along the SW coast of England (Fig. 1). According to the classification of beach response to the 2013/14 extreme storms (Burvingt et al., submitted), these 16 beaches are classified as follows: fully exposed beaches (#3, #5, #6 and #9) ; semi-exposed beaches (#1, #4, #7 and #8); sheltered short beaches (#2, #10, #11 and #13); sheltered long beaches (#12, #14, #15 and #16). They particularly vary in length (from 325 m to 4800 m), in sediment size with 14 beaches composed of sand and two others of shingle (#15, #16), and in dune size when they are present (#1, #3, #4, #5, #7, #8, #9).

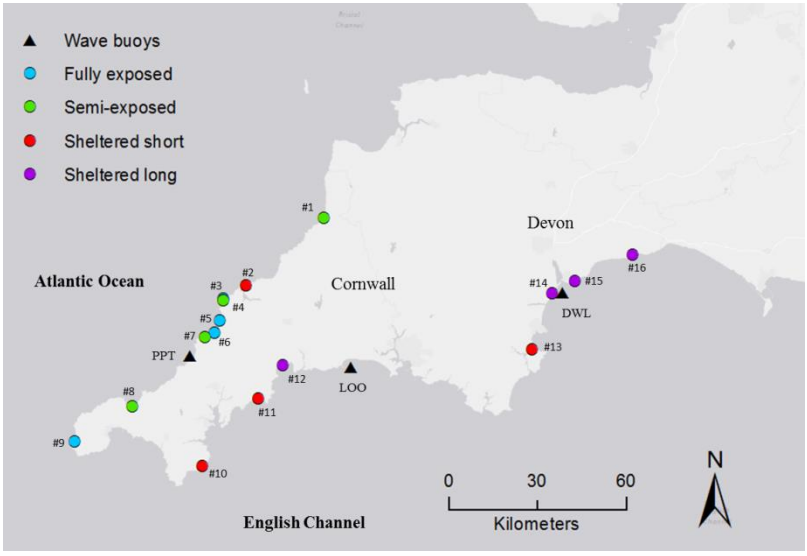

Figure 1. Map of the southwest coast of England. The 16 study sites are coloured according to their storm response classification. Wave buoys are represented with black triangles (PPT = Perranporth, LOO = Looe, DWL = Dawlish).

2.2. *Topographic beach profile and airborne LiDAR dataset*

Annual or bi-annual RTK-GPS surveys have been conducted by the Plymouth Coastal Observatory along the SW coast of England since 2007 (http://southwest.coastalmonitoring.org). Profiles are surveyed in the spring and the autumn at most sites. The dataset of 16 beaches comprises 92 cross-shore profiles and the

minimum, mean and maximum number of profiles per beach is 1, 6 and 17, respectively.
The coastline of SW England is also surveyed by airborne LiDAR, commissioned by the Environment Agency (EA). Different sections of the coast are surveyed in different years, almost always during the spring months, and the whole coast was surveyed in spring 2014 following the extreme events of the winter 2013/2014.

2.3. *Wave buoy dataset*

The coastline of SW England forms a peninsula where the north and south coasts are exposed to different wave regimes. The north coast, largely facing the Atlantic Ocean, is dominantly exposed to swell from NW-W-SW directions, whereas the south coast is facing the English Channel and is dominantly exposed to a mixture of (rarer) SW swell and S-E wind waves. Wave height and period from three wave buoys located offshore along the north and the south coast (Fig. 1) were used to characterise the wave conditions. The buoys are all positioned in relatively shallow water (10-12 m water depth), providing an appropriate representation of the wave conditions at the coast. Perranporth wave buoy on the north coast has recorded waves from 2008 to 2017, whereas Looe and Dawlish wave buoys on the south coast started recording in mid-2009 and 2011, respectively.

3. Net profile and total beach volumes time-series

The 2D profiles surveyed along the different study sites vary in cross-shore length x and are variably spaced from each other along the beach. For each profile, at each survey, the measured topographic values z_x are interpolated every 1 m along the x-axis. Based on the shortest profile, z_x arrays are cut to start and stop at the same landward and seaward x location, respectively. These z_x values are then added together for each profile i to obtain profile sediment volume per unit m width, Q_i:

$$Q_i = \sum_1^N z_x \qquad (m^3.m^{-1}) \tag{1}$$

where N corresponds to the total number of topographic values for each profile i, which is equivalent to the cross-shore length of this profile. For each profile i, the chronologic sequence of bi-annual or annual Q_i values, constitute a time-series of the net volume per unit m width $Q_i(t)$ relative to the start of the survey period ($Q_i(t=0) = 0$).
Where there is limited alongshore variability in beach volumetric changes (*i.e.*, the beach is dominated by cross-shore sediment transport as in response types 1, 2 and 3), the total beach length L is divided into M alongshore lengths L_i. The L_i values depend on the variable alongshore distance between the cross-shore profiles. The $Q_i(t)$ time-series are then summed together and multiplied to the corresponding L_i length, before being divided by the total length of the beach L to obtain the total net volume per unit m width $Q_{tot}(t)$:

$$Q_{tot}(t) = {}^1/_L \left(\sum_i^M Q_i(t) * L_i\right) \qquad (m^3.m^{-1}) \tag{2}$$

To facilitate the comparison between the different beaches and the evaluation of the beach recovery percentages, $Q_i(t)$ and $Q_{tot}(t)$ time-series are normalized according to the 2013/14 net volumetric change per unit meter width:

$$Q'_{tot}(t) = \frac{Q_{tot}(t)}{Q_{tot}(pre) - Q_{tot}(post)} * 100 \qquad (\%) \tag{3}$$

Where $Q_{tot}(pre)$ and $Q_{tot}(post)$, respectively, correspond to the pre-storm and post-storm total net volumes after the beach eroded during the 2013/14. To graphically read the recovery percentages (Fig. 7), the $Q_{tot}'(t)$

are set in a way that $Q_{tot}'(post)$ equals zero ($Q_{tot}'(t) = Q_{tot}'(t) - Q_{tot}'(post)$). The same equation is also used to calculate $Q_i'(t)$ when only net profile volumes are considered instead of the total beach volumes.

4. Wave conditions

Time series of the significant wave height H_s and peak wave period T_p are plotted in Figure 2. The time series of the wave conditions shows a clear seasonal variability with a dominance of large and long waves during winter times (November–March), and smaller and shorter waves during spring and summer months (Fig. 2). At Perranporth on the north coast of Cornwall (Fig. 2c), high H_s values (c. 5 m) can be observed during the 2013/14, 2014/2015 and 2015/16 winters, with relatively smaller H_s values (c. 3 m) from 2008 to 2013 (Fig. 2c). During the 2013/14 winter, H_s values barely drop below 2 m for the entire winter period due to the exceptional series of storms (Fig. 2c). At Looe on the south coast of Cornwall (Fig. 2a), H_s values (c. 4 m) during the 2013/14 and 2015/16 winters clearly stand out over the 2009–2017 period (Fig. 2a). At Dawlish on the south coast of Devon (Fig. 2b), wave conditions are slightly less energetic than at Looe (c. 3 m; Fig. 2b). The 2013/14 and 2015/16 winter at Dawlish also shows the highest H_s values over the 2011–2017 period (Fig. 2b). It is noted that at all three locations, the second- and third-most energetic winters (after 2013/14) were 2015/16 and 2014/15, respectively.

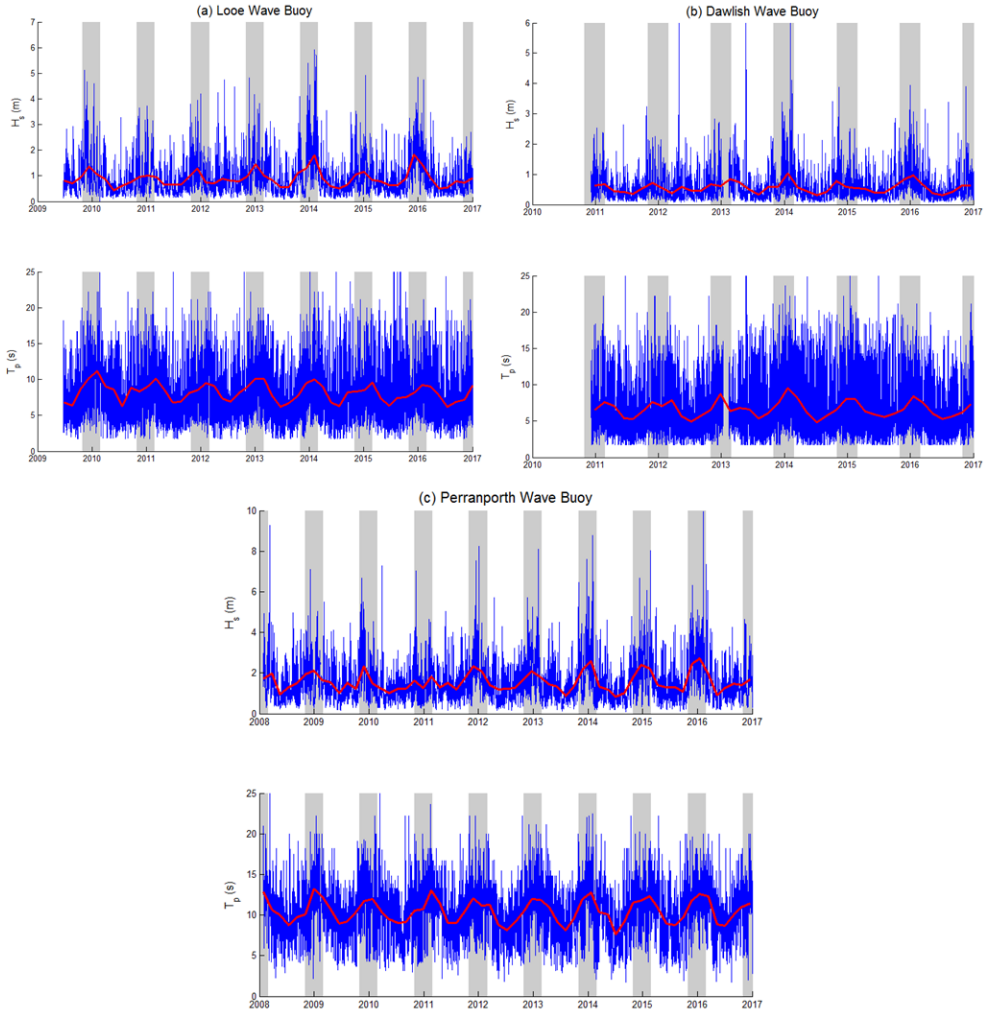

Figure 2. Time-series of hourly (blue) and 8-weeks (red) moving average of significant wave height H_s (top) and peak wave period T_p (bottom) at the three wave buoy locations: (a) Looe, (b) Dawlish and (c) Perranporth. Winter periods (from November to March) are shaded in grey.

5. Storm response, 10-year beach evolution and recovery processes

The classification of beach response to the 2013/14 extreme storms identified four different types of beach response (Burvingt et al., submitted). One example of each of the four different responses were selected (fully exposed beach: Watergate Bay #6; semi-exposed beach: Widemouth #1; sheltered short beach: Broadsands #13; sheltered long beach: Budleigh Salterton #15; see Figure 1). For each of these examples, the storm response, topographic changes and long-term beach evolution are shown by a difference plot based on LiDAR-derived Digital Elevation Models (DEMs), three 2D cross-shore profiles and time-series of $Q_i(t)$ or $Q_{tot}(t)$, respectively (Fig. 3, 4, 5 and 6).

Watergate Bay #6 is located on the north coast of Cornwall (Fig. 1) and is representative of the fully exposed beaches that lost very large amounts of sediment (generally > 100 $m^3.m^{-1}$) during the 2013/14 winter. The LiDAR image illustrates the erosion over the entire intertidal beach area (Fig. 3). This erosion can also be observed along the three profiles selected with a clear vertical lowering of the beach between 2013 (in blue) and 2014 (in red) profiles (Fig. 3). The $Q_{tot}(t)$ time-series indicates that this erosive event was the strongest during the last 10 years and occurred after an extended accretionary period from 2008 to 2010, followed by a relatively stable beach from 2010 to 2013. Following the 2013/14 winter, sediment transport from the lower beach area (c. -2 m) to the upper beach area (c. -1 m and above) can be observed along the 2015 profiles (in black) with the formation of a sand bar at the middle profile (Fig. 3). The 2016 profiles (in green) illustrate slight accretion in comparison to the 2015 profiles concurrent with the flattening of the middle profile (Fig. 3). This beach recovery is captured by the $Q_{tot}(t)$ time-series, which is estimated at almost 40% compared to the pre-storm beach volume in 2013 (Fig. 3).

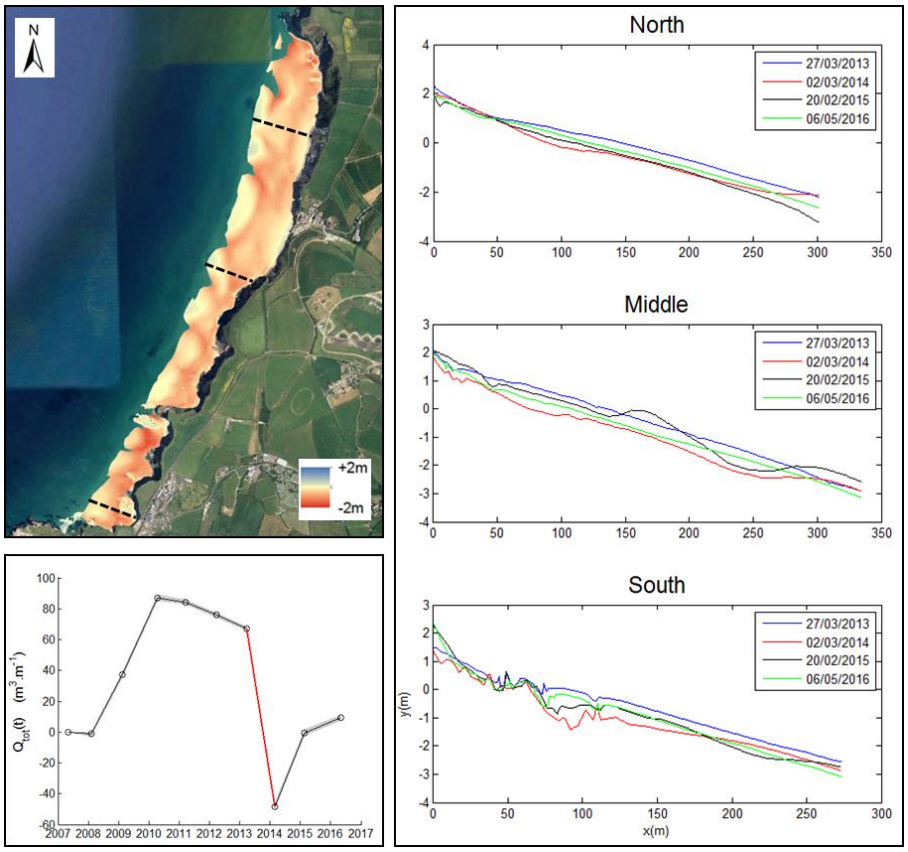

Figure 3. Bed-elevation difference between pre- and post-storm LiDAR DEM; beach profiles for selected periods; and $Q_{tot}(t)$ time-series at Watergate Bay beach #6. The grey envelop around $Q_{tot}(t)$ values represents the standard variation associated with $Q_i(t)$.

Widemouth #1 is also located on the north coast of Cornwall (Fig. 1) and is representative of the semi-exposed beaches that lost large amounts of sediment (50–100 $m^3.m^{-1}$) during the 2013/14 winter. The LiDAR image illustrates erosion over most of the intertidal area with deposition of sand forming a sand bar at the lower area in the middle of the beach (Fig. 4). The formation of this sandbar is captured by the northern profile where strong erosion occurs at the middle of the beach (c. 0 m) and accretion in the lower part (c. -1.5 m) when pre-storm 2013 (blue) and post-storm 2014 (red) profiles are compared (Fig. 4). The middle and southern profiles largely eroded, particularly at the southern profile where the presence of an underlying rock platform has limited the erosion, leading to smaller net volumetric losses $Q_{tot}(t)$. The beach recovery observed along the three 2015 profiles is relatively quick with a large increase in beach volume compared to its post-storm level (Fig. 4). This recovery process ceases, however, during the following 2015/16 winter, which shows beach sediment losses.

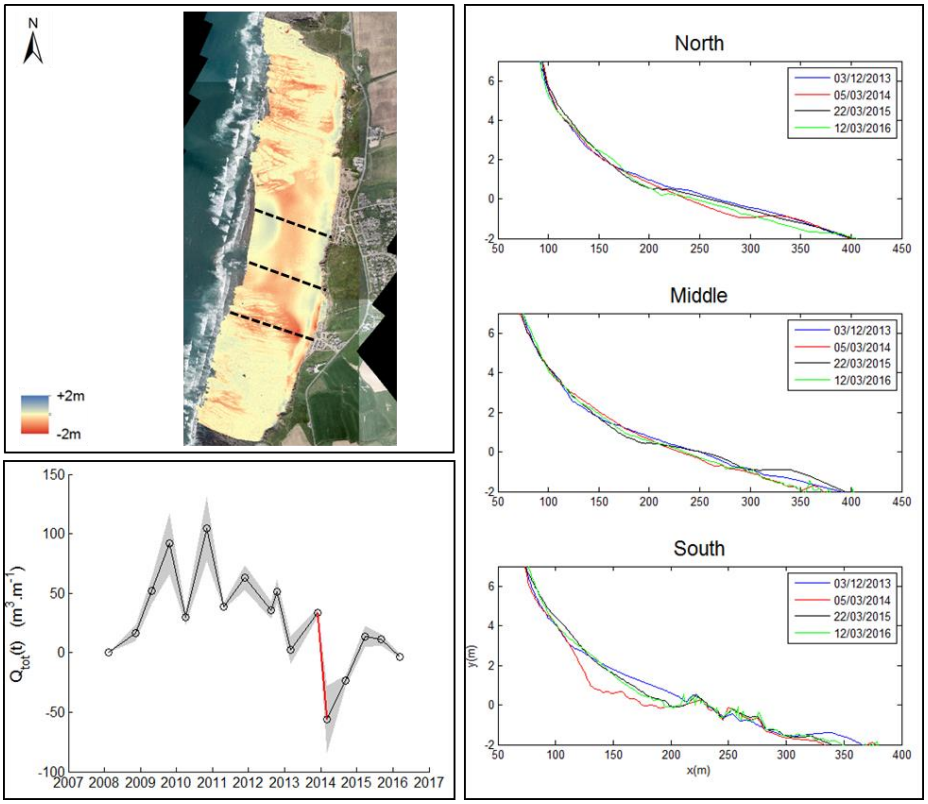

Figure 4. Bed-elevation difference between pre- and post-storm LiDAR DEM; beach profiles for selected periods; and $Q_{tot}(t)$ time-series at Widemouth Bay beach #1. The grey envelop around $Q_{tot}(t)$ values represents the standard variation associated with $Q_i(t)$.

Broadsands #13 is located on the south coast of Devon (Fig. 1) and is representative of the sheltered and short beaches that either lost or gained relatively small volumes of sediment (generally < 25 $m^3.m^{-1}$) during the 2013/14 winter. In contrast to the two previous examples, Broadsands beach accreted during the 2013/14 winter. As shown on the LiDAR image and along the three 2014 profiles (in red), no change occurred on the southern part of the beach facing north, whereas the upper area (c. 1 m) accreted at the middle and northern part of the beach (Fig. 5). The volumetric change time-series $Q_{tot}(t)$ indicates that this accretive period interrupted an erosive period from 2012 to 2013 (Fig. 5). However, following the 2013/14 winter, Broadsands beach kept gaining sediment until the 2016/17 winter when limited erosion occurred (Fig. 5).

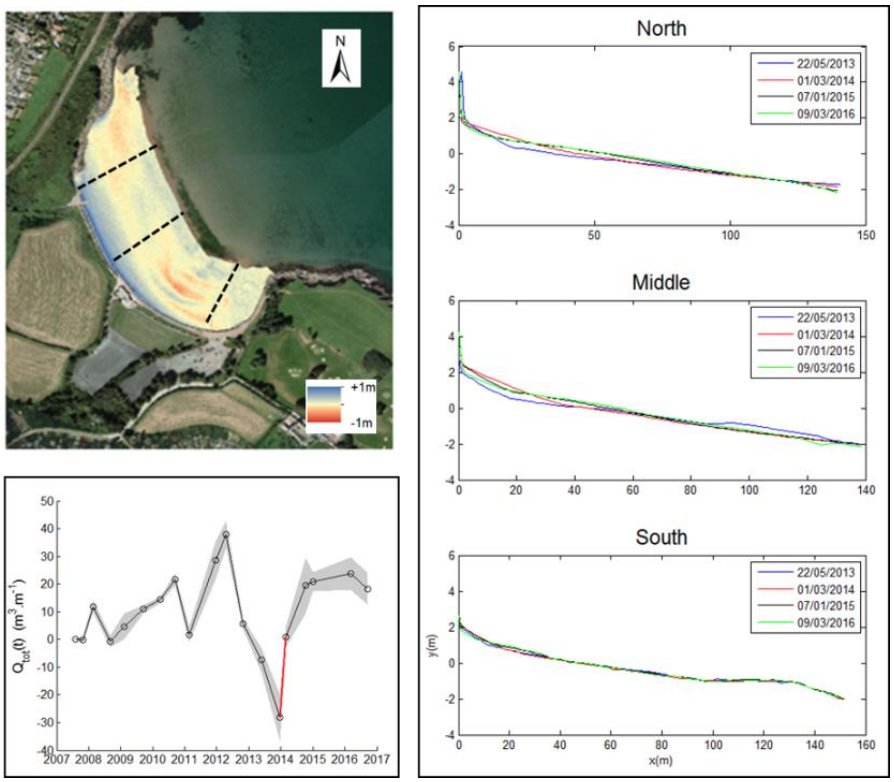

Figure 5. Bed-elevation difference between pre- and post-storm LiDAR DEM; beach profiles for selected periods; and $Q_{tot}(t)$ time-series at Broadsands beach #13. The grey envelop around $Q_{tot}(t)$ values represents the standard variation associated with $Q_i(t)$.

Budleigh Salterton #15 is located on the south coast of Devon (Fig. 1) and is representative of the sheltered and long beaches that rotated horizontally (clockwise) during the 2013/14 winter. The LiDAR image and the three different profiles perfectly illustrate this rotation (Fig. 6). The western part of the beach (profile 63) vertically lowered, whereas the eastern part (profile 18) accreted. Moreover, as can be seen on the LiDAR image, most of the western part that could not been surveyed, due to lack of access, also strongly eroded. Although much variation can be observed along the profile located in the middle of the beach (number 39), this part of the beach seems to act as a pivot point with relatively constant $Q_i(t)$ values. Because of the strong alongshore variability in volumetric change, the total volumetric change is not represented in this case; instead, for each profile the time series of volumetric change $Q_i(t)$ is plotted in Figure 6. The previous observations made for the three profiles can be extrapolated to the set of profiles spread along the beach with slight change in gradation (Fig. 6). More importantly, almost three years later, none of the western profiles seem to have recovered, and some even lost more sediment, whereas the eastern part remained stable or kept accreting.

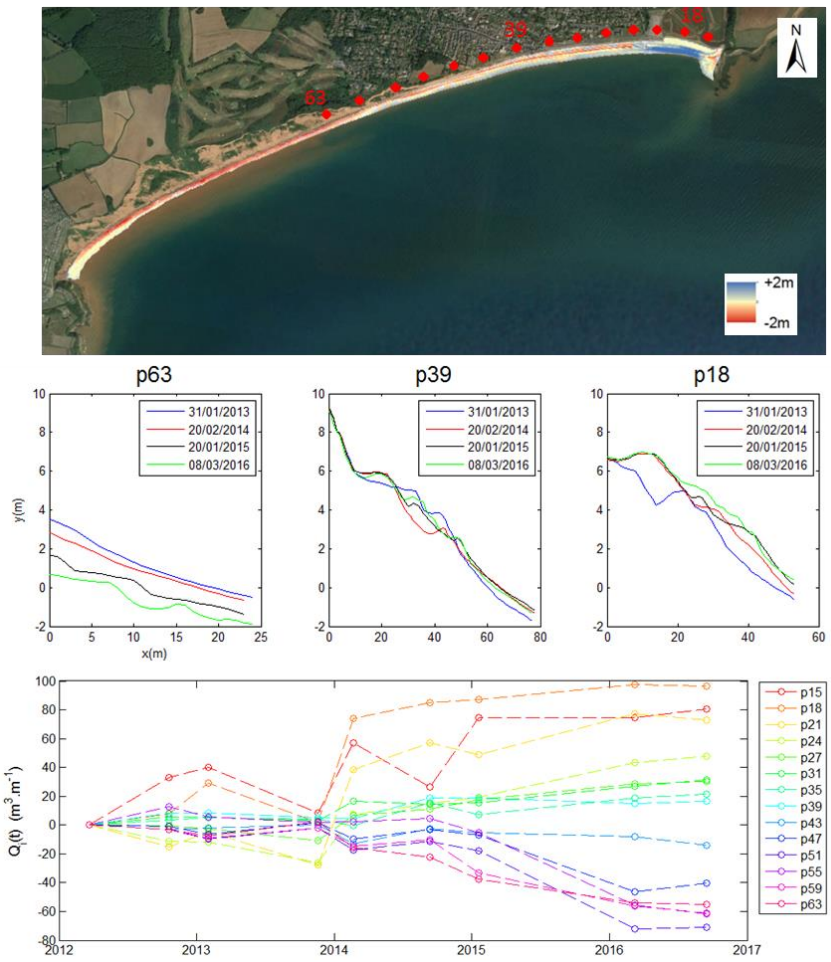

Figure 6. Difference of LiDAR DEMs image, 2D cross-shore profile changes and $Q_i(t)$ time-series at Budleigh Salterton beach #15.

6. Regional variability and wave forcing

Four examples corresponding to four different types of storm response were discussed in the previous section, highlighting the regional variability along the southwest coast of England in terms of beach response during the 2013/14 winter, beach recovery and 10-year volumetric changes. The study was extended to 16 study sites evenly divided among the four different storm responses. The 16 beaches were either annually or bi-annually surveyed, to facilitate comparison between the different time-series and to avoid aliasing, only the late winter-early spring (i.e., February to March) surveys were considered. For beaches that showed little alongshore variability in beach response and significant volumetric loss during the 2013/14 winter, the normalized total net volume time-series $Q_{tot}'(t)$ (Equation 3) was used to enable comparison of the recovery processes (Fig. 7a, 7b and 7c upper panel). For the beaches that gained sediment during the 2013/14 winter, the total beach volume time-series $Q_{tot}(t)$ (Equation 2) was used since that winter only accounted for small volumetric changes (Fig. 7c lower panel). For the beaches that showed large alongshore variability in beach response during the 2013/14 winter, only the volume time-series $Q_i'(t)$ corresponding to profiles located at the beach extremities are plotted (Fig. 7d).

The four fully exposed beaches (#3, #5, #6 and #9), all located on the north coast of Cornwall (Fig. 1), show very similar normalized volume time-series $Q_{tot}'(t)$ (Fig. 7a). An extended period of accretion occurred from 2007 to 2013; normalized sediment volumes increased by approximatively 50% and reached a maximum at the end of 2013. This period was characterized by relatively calm winters in terms of the significant wave height H_s at the Perranporth wave buoy (Fig. 2c). This accretionary period was followed

by very large loss of sediment during the 2013/14 winter (Fig. 7a). High values of H_s (c. 3.5 m) and T_p (c. 15 s) were regularly recorded at Perranporth during this winter. Regarding the recovery process following that energetic winter, the four beaches show some inter-site variability with the return of c. 40 % of the sediment after a year at Watergate Bay #6 and Trenance #5, while Booby's Bay #3 showed no recovery, and Sennen beach #9 continued to erode (Fig. 7a). The 2014/15 and 2015/16 winters also show relatively high H_s and T_p values over these winters (Fig. 2c). The weak recovery of these four beaches is attributed to these relatively energetic winter wave conditions but cannot easily explain the variability between the four beaches.

Also located on the north coast of Cornwall (Fig. 1) and exposed to similar wave conditions (Fig. 2c), the four semi-exposed beaches (#1, #4, #7 and #8) show comparable $Q_{tot}'(t)$ time-series (Fig. 7b). An extended period of accretion occurred from 2007 to 2013 with normalized sediment volumes increasing by approximatively 30-40% over this period and reaching their maximum values at the end of 2013. The 2013/14 winter was also responsible for the largest loss of sediment (Fig. 7b) and, except Widemouth #1 which fully recovered after a year, the three other beaches recovered by c. 30% and this recovery was interrupted by a relatively small loss of sediment in the 2015/16 winter.

The four beaches classified as sheltered and short beaches (#2, #10, #11 and #13) vary in location (Fig. 1) and are consequently exposed to different wave climates. Polzeath #2, located on the north coast of Cornwall, showed a $Q_{tot}'(t)$ time-series similar to the ones observed at the fully and semi-exposed beaches (Fig. 7c). However, being much more embayed and oriented slightly away from the prevailing swell direction (Burvingt et al., submitted), the volumes of sediment lost during the 2013/14 winter were relatively small. This may be one of the reasons why the beach fully recovered and even gained more sediment compare to its pre-storm level by 2015. This post-storm accretion was also interrupted during the energetic 2015/16 winter (Fig. 7c). Porthluney #11 is an embayed beach located on the south coast of Cornwall that also lost a relatively small amount of sediment during the 2013/14 winter. During this winter the largest sediment loss occurred on this beach (Fig. 7c), but the beach fully recovered within a year, before experiencing moderate erosion during the 2015/16 winter. The closest wave buoy at Looe (Fig. 1), representative of the wave conditions in the area, showed higher H_s values during the 2013/14 and 2015/16 compared to the other winters (Fig. 2a), and are likely responsible to these two erosive periods. Alternatively, Coverack #10 and Broadsands #13 show variable total net volumes time-series $Q_{tot}(t)$ from 2007 to 2013, but the two beaches, which are both orientated away from the prevailing swell direction (Burvingt et al., submitted) gained relatively small volumes of sediment (Fig. 7c). Sediment deposition extended during the following two years, reaching the maximum sediment volume at Coverack # 10 in 2016. Looe wave buoy is the closest buoy to these two study sites (Fig. 1) and although it recorded the largest H_s values during the 2013/14 and 2015/2016 winters (Fig. 2a), these two beaches are so sheltered that these wave records are not considered representative of the actual wave conditions.

The last four beaches (#12, #14, #15 and #16), all located on the south coast (Fig. 1), are classified as sheltered and long beaches. They all experienced a clockwise horizontal rotation during that winter, as illustrated on the LiDAR image of Budleigh Salterton #15 beach (Fig. 6). In Figure 7d, beach rotation during the 2013/14 winter can be identified by the two $Q_i'(t)$ time-series from the beach extremities either crossing (Carlyon #12 and Seaton #16) or diverging (Dawlish #14 and Budleigh #15). The $Q_i'(t)$ time-series for Carlyon #12 is the longest and shows that an anti-clockwise rotation happened during the 2008/09 winter. Wave records at Dawlish indicated that the 2013/14 winter was highly energetic compared to the three previous winters (Fig. 2b). Seaton #16 was the most reactive and counter-rotated the following year; Carlyon #12 and Dawlish #14 showed some recovery during that same year; however, Budleigh Salterton #15 showed no recovery at all (Fig. 7d). Any recovery process was interrupted during the 2015/16 winter, when wave conditions recorded at Dawlish (Fig. 2b) were similar to that during the 2013/14 winter: beach rotation was enhanced at Carlyon # 12 and Dawlish #14 beaches, Seaton #16 rotated once again and Budleigh Salterton #15 remained stable (Fig. 7d).

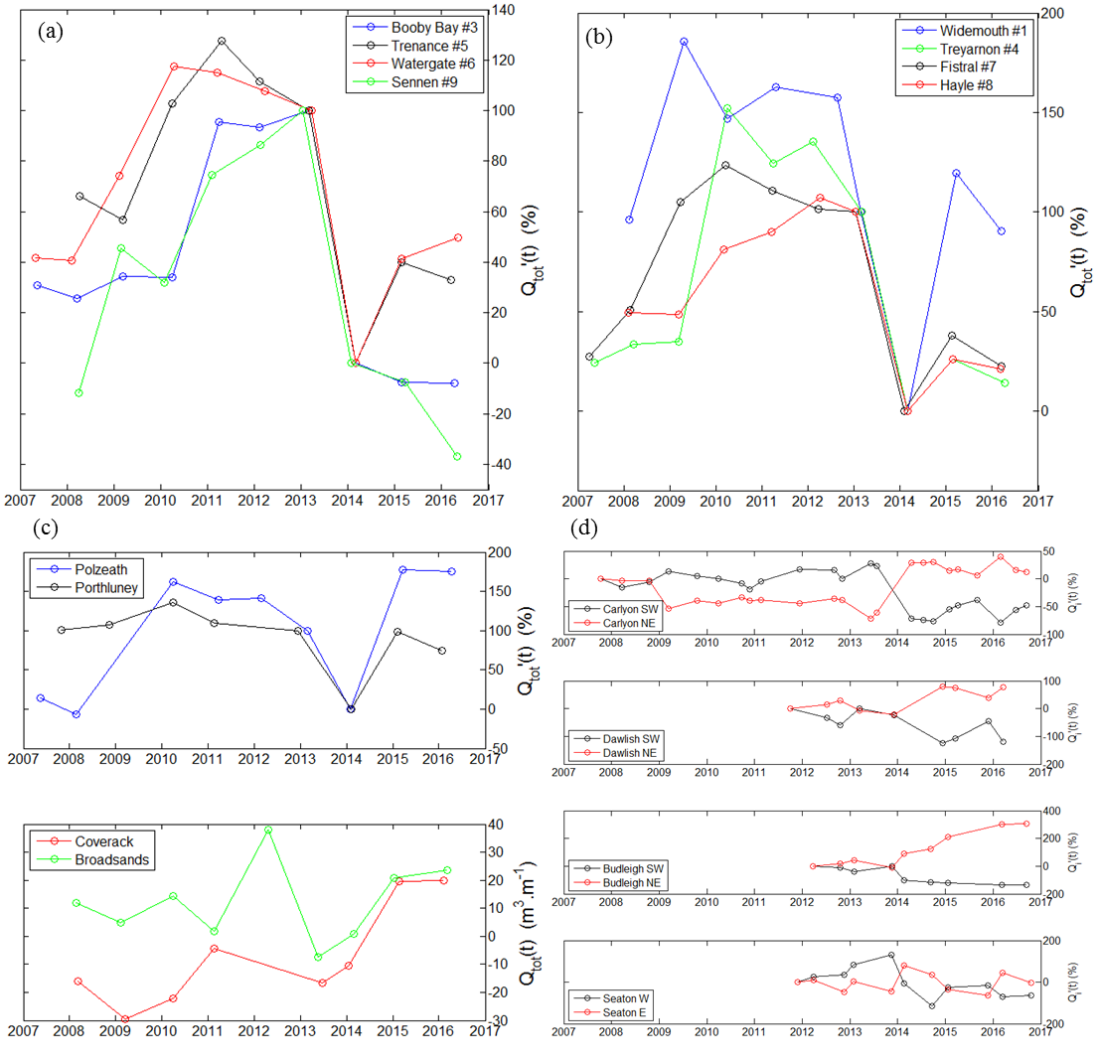

Figure 7. Volume time-series $Q_{tot}'(t)$, $Q_{tot}(t)$ and $Q_i'(t)$ at: (a) fully exposed beaches, (b) semi-exposed beaches, (c) sheltered short beaches and (d) sheltered long beaches.

7. Discussion and conclusions

During the 2013/14 winter, the wave conditions along the southwest coast of England were the most energetic period of the last 60 years (Masselink et al., 2015). These conditions were responsible for variable sediment volumetric changes along this highly diverse coastline, resulting in four types of beach response (Burvingt et al., submitted). This study shows that these storm responses were also inscribed in variable multi-annual volumetric evolution contexts. For the fully and semi-exposed beaches, the 2013/14 winter resulted in the largest loss of sediment for at least the last 10 years. Similarly, other exposed beaches along the Atlantic coastline of Europe also experienced the largest sediment loss for the last 10 or 15 years (Blaise et al., 2015; Castelle et al., 2015). Although the volumes of sediment involved were relatively small, this period also corresponds to the largest volumetric changes at some sheltered beaches.

Although similarities have are found between some of the study sites, this study also demonstrates that beach recovery processes were site-specific. Percentages of recovery after a year vary from 0 (Booby Bay #3) to 100% (Porthluney #11). One beach even experienced even more erosion (Sennen #9 beach), whereas other beaches showed an excess in recovery (Widemouth #1 and Polzeath #2). However, most beaches show some post-storm recovery during 2014 and 2015, and interruption of this recovery process during

2016. Several studies have shown the influence of wave forcing in beach recovery (Pye and Blott, 2008; Barnard et al., 2015; Masselink et al., 2016; Scott et al., 2016; Splinter et al., 2016) and wave records at the three wave buoys along SW England clearly showed that the 2015/16 winter was, like the 2013/14 winter, very energetic. The 2015/16 winter was therefore likely responsible of the weak beach recovery observed at most of the fully exposed, semi-exposed and sheltered long beaches. However, Truc Vert beach along the SW coastline of France was also fully exposed to the 2013/14 storm swells but fully recovered the following year (Castelle et al., 2017). Other factors can also influence beach recovery, like the severity of the storm(s) (Corbella et al., 2012) and the mechanisms involved in beach response to this/these storm(s) (Pardo-Pascual et al., 2014; Scott et al., 2016). In our case, the two main storm responses, characterized by (a) dominant cross-shore sediment transport at fully and semi-exposed beaches located on the north coast and (b) alongshore redistribution of the sediment at sheltered long beaches located on the south coast, surely involve different mechanisms in beach recovery. The recovery process along most of the north coast relies on the mobilisation of relatively deep offshore storm bar deposits (Scott et al., 2016; Phillips et al., 2017). On the south coast, where alongshore redistribution of sediment is the main storm response on the long and sheltered beaches, the recovery processes relies on the occurrence of energtic wave conditions from the opposing wave direction (Pardo-Pascual et al., 2014; Scott et al., 2016). Another factor to be taken into account in beach recovery is the antecedent beach state (Voudoskas et al., 2012). Here, the 10-year beach evolution time-series showed the 2013/14 winter storms occurred when the sediment volume of the fully and semi-exposed beaches were at their maximum for the last 10 years, which would have enhanced the storm response. Moreover, these maximum beach volumes were reached after 3–4 years of relatively calm wave conditions and such a period may be required for a full recovery process. Morpho-dynamic relationships between the beach and the intertidal/subtidal bar (Houser et al., 2015; Brooks et al., 2017; Phillips et al., 2017) and/or sub-aerial dune systems (Suanez et al., 2012; Houser et al., 2015; Castelle et al., 2017) are not considered in this study, but also play an important role in beach recovery processes and need further investigation.

This study showed clear parallels between wave forcing and multi-annual beach evolution. The extreme storms of the 2013/14 winter were responsible of significant morphological changes at many beaches along the SW coast of England. Two years later, many of the beaches that were most affected by the 2013/14 storm waves only showed partial recovery. This study also highlights the existence of beach behaviour that is relatively coherent along the north coast of Cornwall on a multi-annual scale, such as observed along the eastern coast of Australia (Short et al., 2014; Bracs et al., 2016), and reinforces the importance of regional wave forcing in beach morphological evolution and coastal vulnerability (Barnard et al., 2015; Masselink et al., 2016; Scott et al., 2016).

Acknowledgements

The research reported here was funded by the NERC urgency grant ‘Impact of sequence of extreme storms during 2013/2014 winter on southwest coast of England (NE/M004996/1). We would like to thank our two Project Partners, the Plymouth Coastal Observatory (Emerald Siggory) for making available LiDAR and wave data. Additional funding for this project was received from NERC grant NE/N015525/1 (Strategic Highlights Topics).

References

Barnard, P.L., Hubbard, D.M. and Dugan, J.E., 2012. Beach response dynamics of a littoral cell using a 17-year single-point time series of sand thickness. Geomorphology, 139–140: 588–598.

Barnard, P.L., Short, A.D., Harley, M.D., Splinter, K.D., Vitousek, S., Turner, I.L., Allan, J., Banno, M., Bryan, K.R., Doria, A., Hansen, J.E., Kato, S., Kuriyama, Y., Randall-Goodwin, E., Ruggiero, P., Walker, I.J. and Heathfield, D.K., 2015. Coastal vulnerability across the Pacific dominated by El Nino/Southern Oscialltion. *Nature Geoscience*, 8: 801-808.

Birkemeier, W.A., 1979. The effects of the 19 December 1977 coastal storm on beaches in North Carolina and New Jersey. *Shore Beach*, 47: 7-15.

Blaise, E., Suanez, S., Stéphan, P., Fichaut, B., David, L., Cuq, V., Autret, R., Houron, J., Rouan, M., Floc’h, F., Ar dhuin, F., Cancouët, R., Davidson, R., Costa, S. and Delacourt, C., 2015. Bilan des tempêtes de l’hiver 2013-2014 s ur la dynamique du recul du trait de côte en Bretagne. *Geomorphologie Relief Processus Environment*, 21:267-292.

Bracs, M.A., Turner, I.L., Splinter K.D., Short, A.D. and Mortlock, T.R., 2016. Synchronised patterns of erosion and deposition observed at two beaches. *Marine Geology*, 380: 196-204.
Brooks, S.M., Spencer, T. and Christie, E.K., 2017. Storm impacts and shoreline recovery: Mechanisms and controls in the southern North Sea. Geomorphology, 283: 48-60.
Burvingt, O., Masselink, G., Russell, P. and Scott, T., 2016. Beach response to consecutive extreme storms using LiDAR along the SW coast of England. *Journal of Coastal Research*, SI (75): 1052-1056.
Burvingt, O., Masselink, G., Russell, P. and Scott, T., submitted. Classification of beach response to extreme storms. *Geomorphology*.
Castelle, B., Marieu, V., Bujan, S., Splinter, K.D., Robinet, A., Sénéchal, N. and Ferreira, S., 2015. Impact of the winter 2013-2014 series of severe Western Europe storms on a double-barred sandy coast: beach and dune erosion and megacusp embayments. Geomorphology, 238: 135-148.
Castelle, B., Bujan, S., Ferreira S. and Dodet, G., 2017. Foredune morphological changes and beach recovery from the extreme 2013/2014 winter at a high-energy sandy coast. *Marine Geology*, 385: 41-55.
Choowong, M., Phantuwongraj, S., Charoentitirat, T., Chutakositkanon, V., Yumuang, S. and Charusiri P., 2009. Beach recovery after 2004 Indian Ocean tsunami from Phang-nga, Thailand. *Geomorphology*, 104: 134-142.
Corbella, S. and Stretch, D.D., 2012. Shoreline recovery from storms on the east coast of Southern Africa. *Natural Hazards and Earth System Sciences*, 12: 11-22.
Houser, C., Wernette, P., Rentschlar, E., Jones, H., Hammond, B. and Trimble, S., 2015. Post-storm beach and dune recovery: Implications for barrier island resilience. *Geomorphology*, 234: 54-63.
Masselink, G., Scott, T., Davidson, M., Russell, P. and Conley, D., 2015. The extreme 2013/2014 winter storms: hydrodynamic forcing and coastal response along the southwest coast of England. *Earth Surface Processes and Landforms*, 41: 378-391.
Masselink, G., Castelle, B., Scott, T., Dodet, G., Suanez, S., Jackson, D. and Floc'h, F., 2016. Extreme wave activity during 2013/2014 winter and morphological impacts along the Atlantic coast of Europe. *Geophysical Research Letter*, 43: 2135–2143.
Pardo-Pascual, J.E., Almonacid-Caballer, J., Ruiz, L.A., Palomar-Vazquez, J. and Rodrigo-Alemany, R., 2014. Evaluation of storm impact on sandy beaches of the Gulf of Valencia using Landsat imagery series. *Geomorphology*, 214: 388-401.
Phillips, M.S., Harley, M.D., Turner, I.L., Splinter, K.D. and Cox R.J., 2017. Shoreline recovery on wave-dominated sandy coastlines: the role of sandbar morphodynamics and nearshore wave parameters. *Marine Geology*, 385: 146-159.
Poate, T., Masselink, G., McCall, R., Russell, P. and Davidson, M., 2015. UK storms 2014: gravel beach response. *Proceedings Coastal Sediments*, ASCE, San Diego, USA.
Pye, K. and Blott, J.S., 2008. Decadal scale variation in dune erosion and accretion rates: An investigation of the significance of changing storm tide frequency and magnitude on the Sefton coast, UK. *Geomorphology*, 102: 652-666.
Scott, T., Masselink G. and Russell P., 2011. Morphodynamic characteristics and classification of beaches in England and Wales. *Marine Geology*, 286: 1-20.
Scott, T., Masselink, G., O'Hare, T., Saulter, A., Poate, T., Russell, P., Davidson, M. and Conley, D., 2016. The extreme 2013/2014 winter storms: Beach recovery along the southwest coast of England. *Marine Geology*, 382: 224-241.
Short, A.D., Bracs, M.A. and Turner, I.A., 2014. Beach oscillation and rotation: local and regional response at three beaches in southeast Australia. *Journal of Coastal Research*, 66: 712-717.
Splinter K.D., Turner, I.L., Reinhardt, M. And Ruessink, G., 2016. Rapid adjustement of shoreline behaviour to changing seasonlity of storms: observations and modelling at an open-coast beach. *Earth Surface Processes and Landforms*.
Suanez, S., Cariolet, J.M., Cancouet, R., Ardhuin, F. and Delacourt, C., 2012. Dune recovery after storm erosion on a high-energy beach: Vougot Beach, Brittany (France). *Geomorphology*, 139-140: 16-33.
Thom, B.H. and Hall, W., 1991. Behaviour of beach profiles during accretion and erosion dominated period. *Earth Surface Processes and Landform*, 16: 113–127.
Turner, I.L., Harley, M.D., Short, A.D., Simmons, J.A, Bracs, M.A., Phillips, M.S. and Splinter, K.D., 2016. A multi-decade dataset of monthly beach profile surveys and inshore wave forcing at Narrabeen, Australia. *Science Data 3*, (160024).
Vousdoukas, M.I., Almeida, L.P.M. and Ferreira, O., 2012. Beach erosion and recovery during consecutive storms at a steep-sloping, meso-tidal beach. *Earth Surface Processes and Landforms*, 37: 583-593.
Yu, F., Switzer, A.D., Lau, A.Y.A, Yeung, H.Y.E., Chik, S.W., Chiu, H.C., Huang, Z. and Pile, J., 2013. A comparison of the post-storm recovery of two sandy beaches on Hong Kong Island, southern China. *Quaternary International*, 304: 163-175.